Sulfurizing and selenizing metal films in ultra-high vacuum by hydride gas kinetic control

by
Xavier D. Luhman

Submitted to the
Department of Materials Science & Engineering
in Partial Fulfillment of the Requirements for the Degree of

Bachelor of Science

at the

Massachusetts Institute of Technology

June 2019

Signature of Author……
Department of Materials Science & Engineering
April 26, 2019

Certified by……
Rafael Jaramillo
Assistant Professor of Materials Science & Engineering
Thesis Supervisor

Certified by……
Juejun Hu
Associate Professor of Materials Science & Engineering
Chairman, Undergraduate Comittee

Abstract

Molecular beam epitaxy (MBE) is an important, well-established method for creation of thin films. The addition of gaseous sources of hydrogen sulfide and hydrogen selenide is not currently a well-documented or common modification to such systems. While the thermodynamics of using such sources for the production of various chalcogenide thin films are favorable, the actual results thus far do not demonstrate the desired outcome. This indicates that the kinetics of the desired reactions are inhibiting the process. Compared to oxygen, reactions involving sulfur and selenium are slow. In order to ensure that the hydride gases have the opportunity to react as desired, it is necessary to keep the system free of oxygen and to maximize the collisions of gas molecules with the substrate. The first requirement should be achieved simply by using MBE for the process. The second requirement is not provided for in a typical MBE system. Thus, modifications are necessary to increase the reaction rate of the gases, namely by extending the source lines to be closer to the substrate. This thesis addresses the design process for tubing inserts in an existing MBE system.

Acknowledgements

I would like to thank Professor Rafael Jaramillo for all of his guidance and advice in the process of this project. I would also like to thank Kevin Ye and Stephen Filippone for their advice and assistance in materials selection and sourcing, in particular.

Table of Contents

I. Introduction and Background

Bell Telephone Laboratories was widely known for being the source of a variety of scientific and technological advancements. Among these advancements was the technique known as molecular beam epitaxy (MBE).[1] MBE is a synthesis method that allows for detailed control over the growth of semiconductor thin films. MBE growth of III-V and group-IV materials is well-developed, dating back decades.[2]

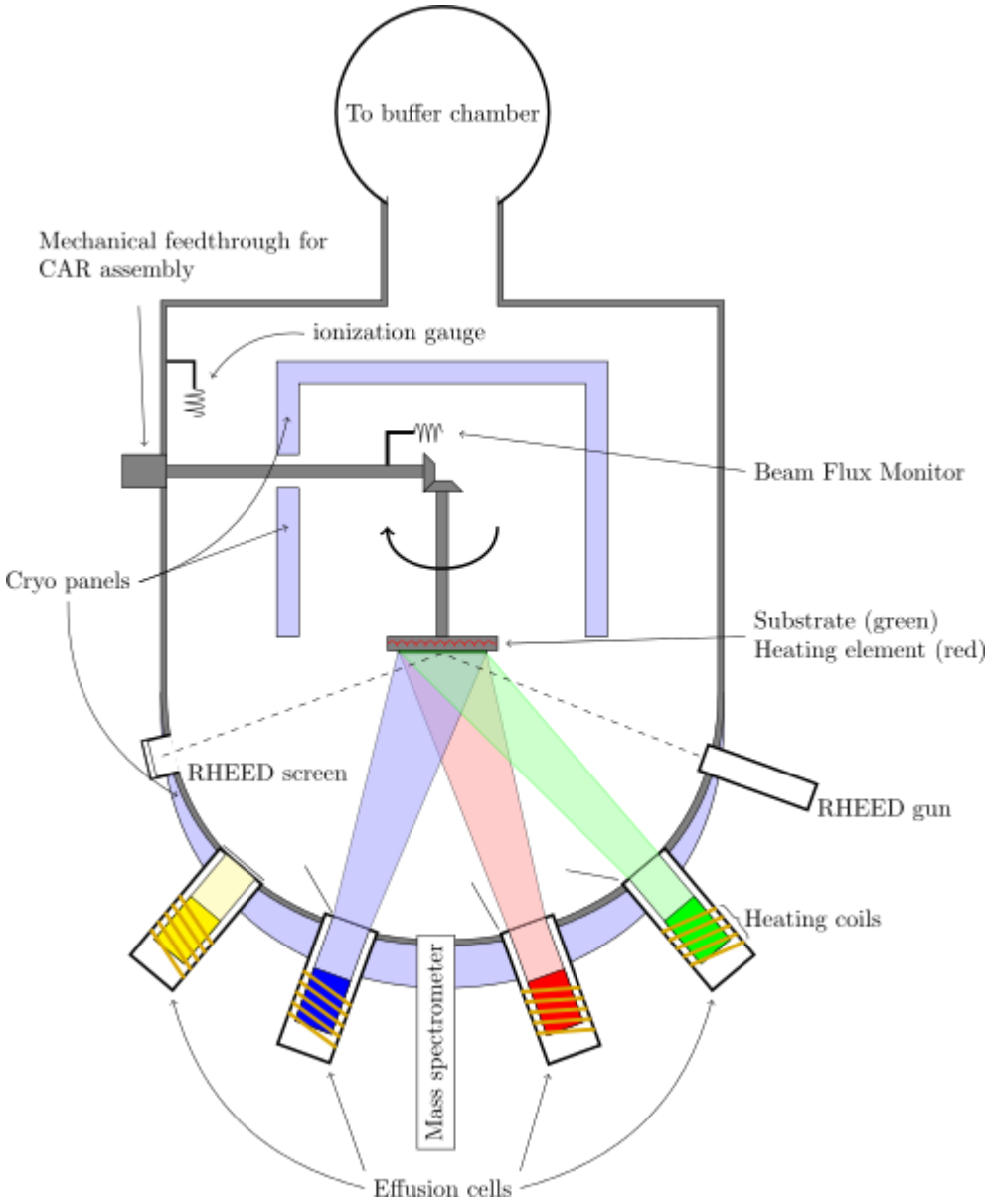

***Fig. 1**, Generic diagram of an MBE system*

Typical MBE systems[3] use crucibles of high-purity elements heated to evaporation or sublimation as the source of atoms (effusion cells). Shutters at the openings of the effusion cells are used to control which sources are in use at a given point in the deposition process. These methods are considered predictable and well-established.

In contrast, the use of hydride gas sources to grow sulfide and selenide films presents new challenges, notably including control over the reactivity of the sulfur and selenium precursors (H_2S and H_2Se, respectively). Although the thermodynamic conditions are favorable for film growth, even with hydride gas pressures as low as 10^{-6} torr, the kinetics of sulfurization and selenization are unfavorably slow.

The Jaramillo Group's MBE system is composed of a variety of instruments. The curved bottom has five ports for traditional effusion cell sources, with fins to keep the beams separated. The bottom also has two gas sources, one for each of the hydrides previously mentioned, and a port for a plasma source. Two large ports extend from the main body parallel to the floor and perpendicular to each other, though at different heights; one is where the vacuum source is attached, and the other is for the electron beam evaporator, a device that allows for the evaporation of materials not suited to the typical effusion cell evaporation. Many smaller ports along the sides connect to or hold devices such as the RHEED gun, RHEED screen, quartz crystal microbalances matched to individual sources, and the residual gas analyzer (RGA).

Typical operating conditions include a vacuum rate around 1000 L/s, an elevated substrate temperature (up to 1000 C), and activation of one or more sources as appropriate for the desired film. When the gas sources are used, the mass flow rate may be anywhere between 0.100 sccm and 1.00 sccm, depending on the desired chalcogenide concentration.

The MBE chamber currently in use in the Jaramillo Lab has not performed as desired when using H_2S or H_2Se to incorporate sulfur and selenium into thin films. Based on film composition data, and gas cracking data obtained using an RGA, it was hypothesized that the in-vacuum gas injector sources are too far away from the substrate to result in frequent enough collisions for cracking to separate the S or Se from the hydrogen, and to incorporate the chalcogen atoms into the film by reacting with the arriving metal atoms.

II. Materials/Methods

II.1 Computer simulation

After the initial determination that the original gas tubing was insufficient for the desired level of sulfur and selenium incorporation, it was proposed that the tubing simply be lengthened. As the distance from the tube increases, the expected flux of gas particles through a given plane decreases, since the particles diffuse into less concentrated areas. By moving the outlet of the gas tubes closer to the substrate, the flux of particles at the substrate would be higher. Between the temperature of the substrate and impact with the substrate itself, increased flux of particles would result in more chalcogenide incorporation. Therefore, an extension of the extant tube was a logical solution. While this modification was being created and installed by other members of the Jaramillo Group, I was assigned to simulate the chamber and the modifications to see how much of a change could be reasonably expected.

On the advice of Mike Galtry of Edwards Vacuum, who noted that the vacuum of the chamber resulted in mean free paths long enough to simulate with discrete particles, the program MolFlow+, created by CERN, was used[4]. MolFlow+ uses Monte Carlo simulation methods to model the movements of particles in a high vacuum environment. Systems can be defined using either simple geometries included with the program or by importing an outside STL file with the desired system.

Due to the nature of even a simplified version of the chamber (a cylinder with a rounded bottom), the system was modeled in SolidWorks and imported. In order to model a system in MolFlow+, facets (various continuous polygons or circles) must be assigned properties like desorption rates or vacuum rates. Since STL files are composed of a large number of triangles,

facets representing the outlet of the gas tube and the opening of the vacuum were created within MolFlow+ in the appropriate locations.

In addition to the gas and vacuum sources, it was necessary to create a method to determine the effects on the substrate. It was decided that the one-directional pressure at the

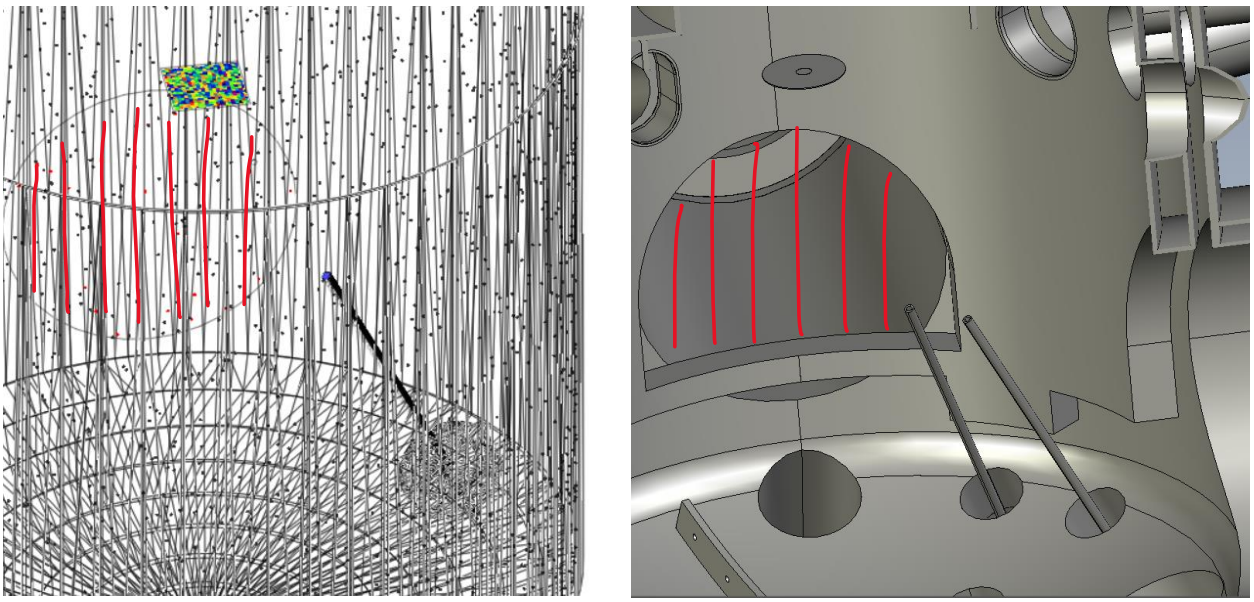

Fig. 2 *Illustration of simplified system in MolFlow+ (left) and more complete system in eDrawings (right). Substrate is at the top in both images; the red lines indicate the mouth of the vacuum; and the gas source is evident in the lower right. (Model courtesy of Mantis Deposition Ltd.)*

substrate plane would be a sufficient analogue to the flux at the same location. While the substrate is typically circular in reality, the program only produced visible textures (color squares) on facets that were rectangular, so the substrate plane was represented using a square.

The pressure at the substrate alone would have been unsuitable for comparison without a reference point, so additional pressure facets were placed along the centerline of the chamber, at the bottom of the chamber, and in roughly the same location as the system's actual pressure gauge. Taking numbers from the additional pressure sensors would allow appropriate contextualization of the increase in pressure at the substrate.

The pressure sensors also served as a method to check that the program functioned as expected. According to the operating manual, MolFlow+ calculates pressure based on recorded

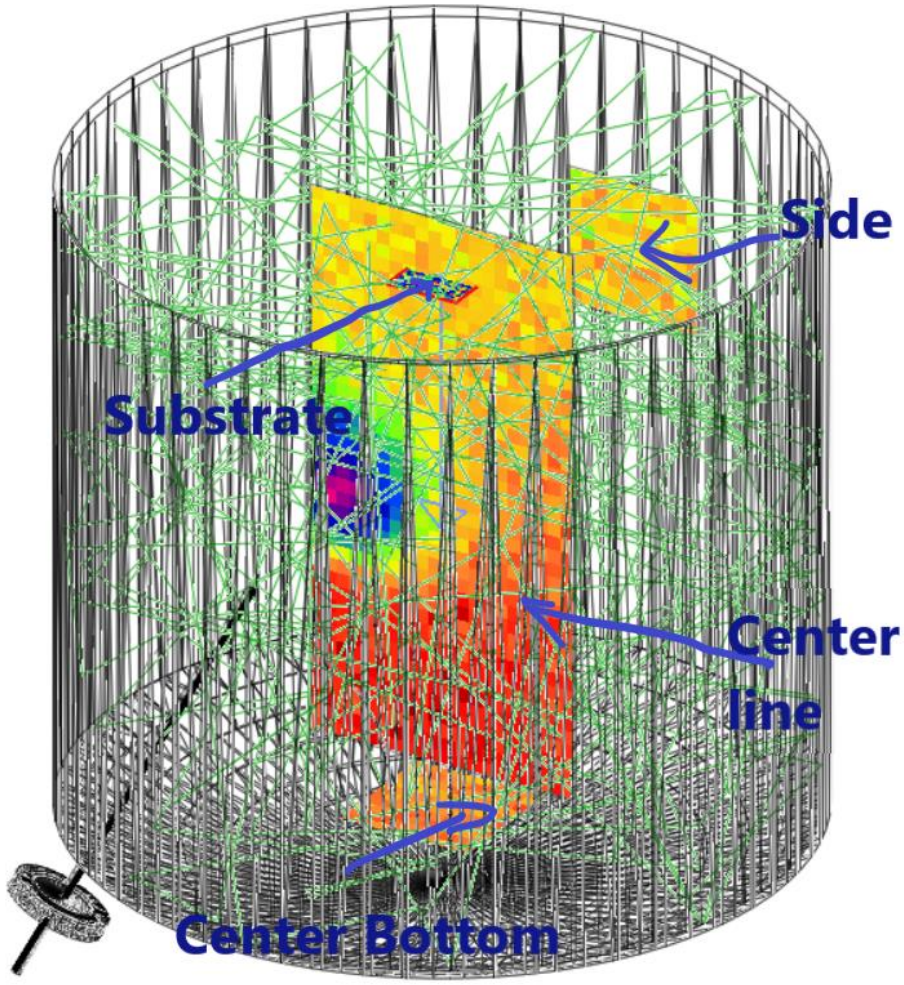

Fig. 3 *An example of a post-simulation view with the original source. Points of note include that the colors on the substrate plane do not demonstrate any defined gradient.*

collisions. Chamber pressure could be calculated independently given the rate of vacuum and the rate of mass flow from the gas source (equation below) and compared to verify the reliability of the program.

$$\frac{Mass\ flow\ rate\ (mbar*\frac{L}{s})}{Vacuum\ pumping\ speed\ (\frac{L}{s})} = Pressure\ (mbar) \quad (1)$$

For a mass flow of 1.00 sccm (0.0169 mbar*L/s) and a pumping speed of 1000 L/s, MolFlow+ reported an average pressure of 1.69E-05 mbar at the side gauge position, exactly as expected, with a standard deviation of 1.43E-07 mbar. Thus, the program is proven reliable.

Interpretation of the colormaps for the substrate and pressure gauge facets has not been necessary for the examples thus far. However, the colormaps are more important in section III.1, so a brief explanation will be given here.

When the colormap is tracking the same property on multiple facets, as it is in the subsequent experiments, all textured facets will use the same scale for the colormap. The colormaps of two separate simulations, however, will not have the same scale. The colors are relative to the detected maximum and minimum in a simulation and tend to change over time, particularly in the beginning stages of a simulation. The colors serve mostly as an easy form of pattern recognition and to provide some visual result of an otherwise numerical data set. The lowest pressures appear black, then move along the color spectrum to red, orange, yellow, green, blue, violet, and pink, should the program decide that the differences are large enough. As such, it is impractical to provide a proper scale or legend for the colormaps seen in section III.1; rather, it will be noted what the maximum and minimum pressures were for a particular experiment, which should provide some degree of reference.

One parameter that was not utilized in replicating actual conditions in the system was temperature. It is possible to set individual facets to different temperatures in MolFlow+. The system is host to a variety of temperatures, with the substrate and surrounding area heated to several hundred degrees Celsius and the cryopanel cooling other parts. For consistency, all facets were left at 293.15 K.

When conducting simulations to collect data, a particular simulation would be run for a minimum of ten minutes to ensure that the system reached an equilibrium. Using tools included in the program, the pressure gradient data was saved as text files and transferred into Microsoft Excel for processing and analysis.

II.2 Part Design

The two parts, one for the hydrogen sulfide source and one for the hydrogen selenide source, were designed in SolidWorks. While the simulations (addressed later) led to the conclusion that a linear injector was most desirable, the location of the sources was only one part of the criteria for the design. It was necessary for the tubing to avoid various key locations in the system, and thus went through a variety of iterations.

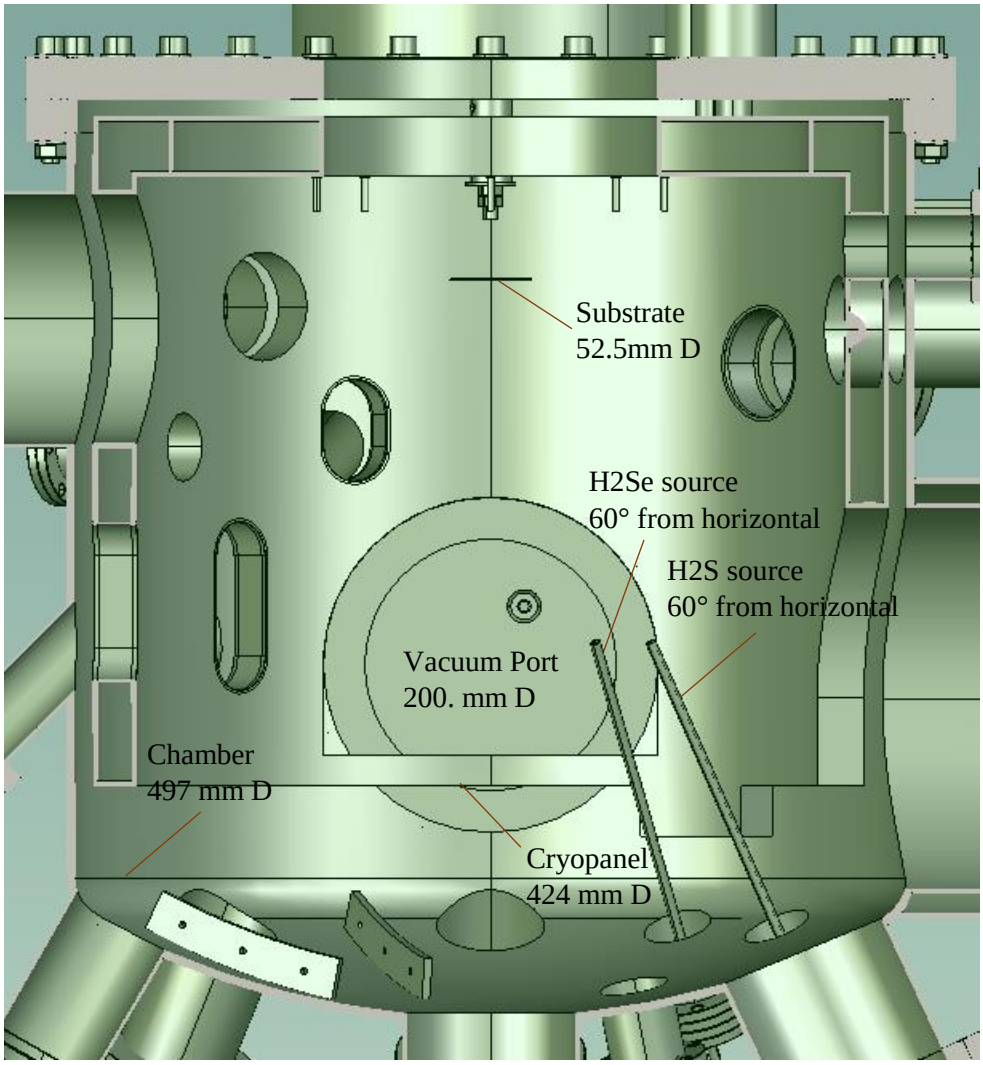

Fig. 4, *Select dimensions and angles of the Jaramillo Lab's MBE system*

The general criteria for the path of the tubing included avoiding a port directly above the original source lines, avoiding the post and plane of the substrate shutter, and making sure to be

wide of the substrate holder itself, which has an outer diameter of 10 cm[5]. It was also vital that the linear injector portion itself be appropriately angled relative to the substrate. The center lines of the holes needed to be directed at the center of the substrate in order to ensure maximum flux. This would be achieved by making the center line of the linear injector tangent to an imaginary circle concentric to the substrate.

II.3 Materials Selection

Due to the corrosive nature of the gases being used in the MBE system, as well as the high temperatures (up to 1000 °C), of concern from the beginning was the material from which the tube would be made. The tubing already in the system is made of molybdenum, as was the extension temporarily installed, but molybdenum is generally unsuitable for complex fabrication and expensive as well.

The initial solution to this was to make the majority of the tubing out of some variety of stainless steel, which would be able to handle the gases but not the high temperatures, while the part closest to the substrate, where it would be hottest, would be made of a different, likely more expensive, material. These two parts would be welded together.

However, this was ultimately dismissed due to a combination of lack of availability of the candidate materials, changes in the design, and the timeline of the project, all of which will be discussed in III.3.

III. Results and Discussion

III.1 Computer Simulation

It was proposed that the extension of molybdenum tubing would add approximately 100 mm to the length of the gas tubing, placing the gas source approximately 150 mm from the substrate. The results of simulations for this distance are included in the following table.

Table 1. *Data for simple extension simulations, modelling actual changes made to the system*

Parameters (distance from substrate, flow rate)	Substrate pressure (mean ± standard deviation)	Chamber pressure (mean ± standard deviation)
250mm, 1 sccm	1.77E-05 ± 6.20E-07 mbar	1.69E-05 ± 1.43E-07 mbar
250mm, 0.1 sccm	1.77E-06 ± 5.56E-08 mbar	1.69E-06 ± 1.21E-08 mbar
150mm, 1 sccm	2.36E-05 ± 2.07E-06 mbar	1.69E-05 ± 1.48E-07 mbar
150mm, 0.1 sccm	2.36E-06 ± 2.15E-07 mbar	1.68E-06 ± 1.56E-08 mbar

As seen in Table 1., the overall chamber pressure, measured at the side gauge location, remained consistent for a given flow rate, regardless of the distance of the source from the substrate, while the pressure at the substrate had a notable increase for the closer location. However, this increase is of relatively small magnitude, less than a 50% increase.

A 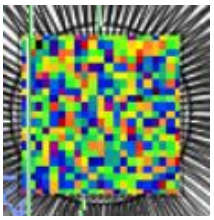 ***B*** 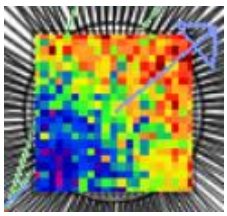

Fig. 5, *Substrate planes showing pressure variations after approx. 10 min of simulation with the source* ***A*** *in its original position* ***B*** *with a 100mm extension; Max/Min (mbar):****A*** *1.91E-05/1.57E-05* ***B*** *2.93E-05/1.66E-05*

Figure 5 shows the visual data obtained from the substrate pressure plane in two different simulations. With the original gas source, the pressure is highly inconsistent, as is expected due to diffusion over the distance from the source to the substrate. The extended source demonstrates an obvious gradient, where red is lower pressure and purple is higher pressure, with the highest pressures in the corner closest to the source. From the min and max pressure values, it is clear that the gradation of the colors is different for each simulation. A bright blue square on A must have a lower pressure value than one on B, but the gradations still serve as an illustration of the effect of moving the source point.

Both the graphical and numerical data demonstrated a marked increase in particle flux at the substrate when the source was extended. This was further supported by the results of operation in the MBE before and after the extension. Measurements were taking using a residual gas analyzer, a type of mass spectrometer. A higher ratio of hydrogen to hydrogen sulfide indicates more cracking of the gas and thus a higher likelihood that sulfur will incorporate into the thin film being deposited on the substrate. This follows from this decomposition

$$H_2S_{(g)} \rightarrow H_{2(g)} + S_{(s)} \quad (2)$$

and assumes the sulfur is more likely to have incorporated in to the film rather than accumulated on other surfaces, for instance. Figure 6 shows a noticeable, but still relatively small, increase in cracking. This increase was considered unsatisfactory.

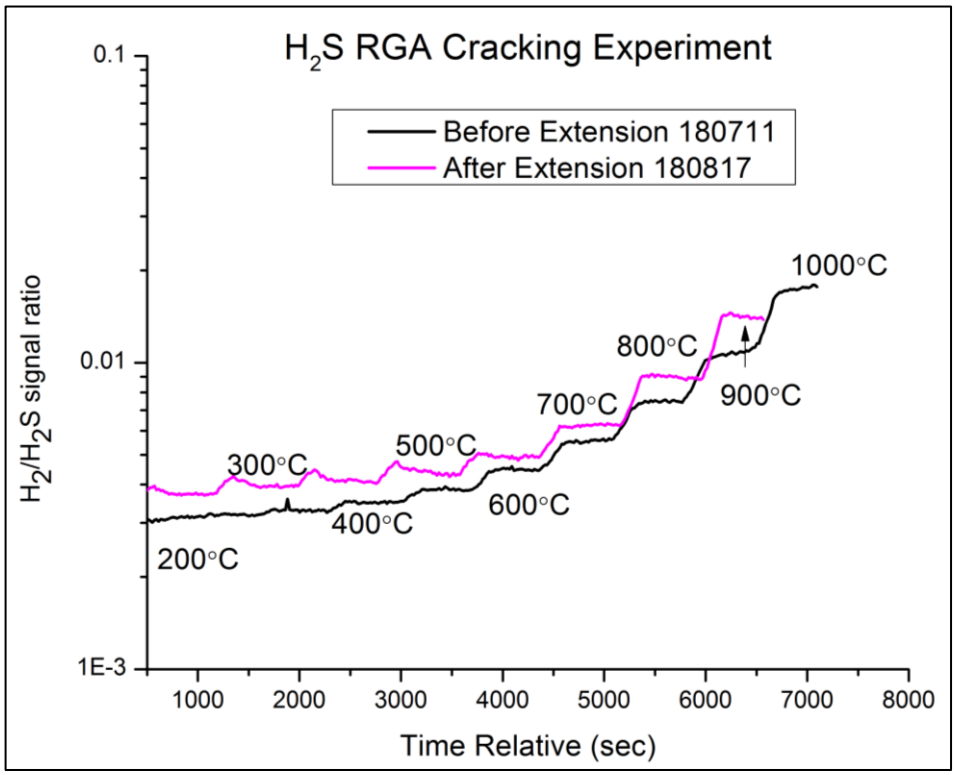

Fig. 6, *Results of MBE deposition runs before and after extension, measured as a ratio of hydrogen to hydrogen sulfide gas signal, where higher ratios are preferred, as per equation 2*

Between the simulation and actual results, it was determined that the simple extension was insufficient. To better understand how the distance from the source to the substrate affected the flux of particles, a series of simulations were run, where the source was moved closer to the substrate in increments of 50 mm. The original source location was 250 mm from the substrate, so source-substrate distances of 200 mm, 150 mm (the actual extension), 100 mm, and 50 mm were also simulated. The results are presented below, numerically in Table 2. and graphically in Figures 7 and 8.

Table 2. *Results of simulations moving the source closer to the substrate, flow rate 1 sccm*

Distance from substrate (mm)	Substrate pressure in mbar (mean ± standard deviation)	Chamber pressure in mbar (mean ± standard deviation)	Difference (mean ± standard deviation)
250	1.77E-05 ± 6.20E-07	1.69E-05 ± 1.43E-07	7.57E-07 ± 6.37E-07
200	1.84E-05 ± 7.45E-07	1.70E-05 ± 1.69E-07	1.41E-06 ± 7.64E-07
150	1.97E-05 ± 9.85E-07	1.69E-05 ± 1.43E-07	2.83E-06 ± 9.96E-07
100	2.36E-05 ± 2.07E-06	1.69E-05 ± 1.48E-07	6.73E-06 ± 2.08E-06
50	3.93E-05 ± 1.09E-05	1.67E-05 ± 1.76E-07	2.26E-05 ± 1.09E-05

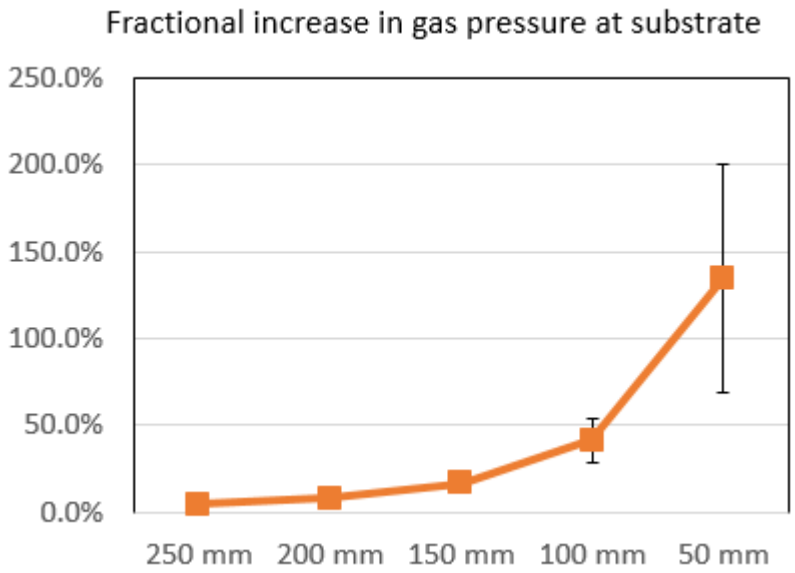

Fig. 7*, fractional increase in pressure at substrate over a range of source-substrate distances*

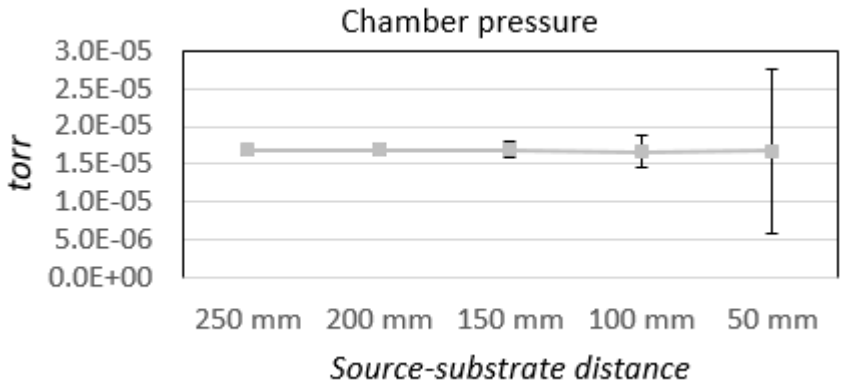

Fig. 8*, chamber pressure over a range of source-substrate distances, largely consistent; error bars relate to standard deviation*

From this series of simulations, it was clear that the sources needed to get much closer to the substrate to have the desired results. However, the structure of the chamber and the need for clear paths for sensors, such as the RHEED and various quartz crystal microbalances, and moving parts prevented a simple linear extension of the existing source lines.

Instead, it was suggested that a ring of sources, like a tube with many holes in the side, or a linear injector might be a viable alternative. To confirm this, three simulations were conducted: a full ring of sources 20 degrees apart with a radius of 3 cm, 2.5 cm below the substrate; a half ring of sources 20 degrees apart with a radius of 3 cm, also 2.5 cm below the substrate; and a linear injector with eight holes, about 2 cm below the substrate. Numerical and visual results presented in Table 3 and Figure 9, respectively.

Table 3. *Results of simulations testing geometry changes, total flow rate 1 sccm*

Geometry	Substrate pressure in mbar (mean ± standard deviation)	Chamber pressure in mbar (mean ± standard deviation)	Percent increase
Ring	3.93E-05 ± 3.49E-06	1.70E-05 ± 2.02E-07	132%
Half ring	3.95E-05 ± 1.31E-05	1.69E-05 ± 9.23E-08	133%
Linear injector	4.00E-05 ± 1.79E-05	1.69E-05 ± 1.86E-07	137%

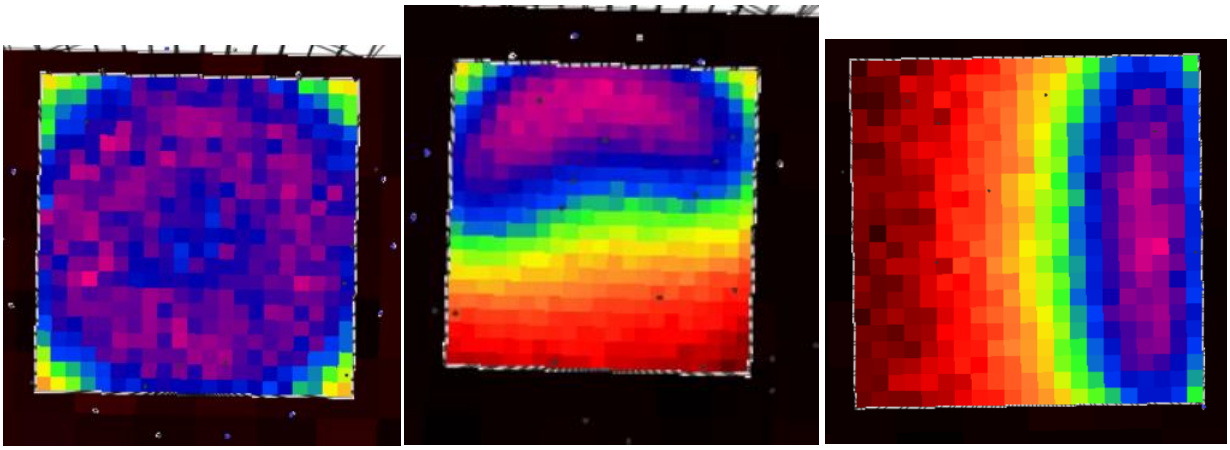

Fig. 9*, substrate pressure gradients, from left to right, ring, half ring, linear;*
Max/min (mbar) from left to right:
4.59E-05/1.65E-05, 7.66E-05/1.65E-05, 6.23E-05/1.67E-05
(in all instances the max is found on the substrate and the min on the gauge)

All three alternate geometries produced promising increases in simulations, with the ring being the most obviously uniform and the linear injector having the widest gap between high and low pressures on the substrate (as seen by the near black squares and the pink squares). However, the uniformity is of low concern compared to increase in average pressure, given that the substrate holder is designed to rotate the substrate regardless of the uniformity of the gas flow.

Since the linear injector was both the simplest geometry (in terms of fabrication needs) and had the highest increase in pressure, it was selected as the best candidate to actually be designed, created, and installed in the system.

One last bit of simulation was conducted during the process of designing the actual parts, where it became necessary to determine how important the vertical distance between the holes and the substrate was. Initial designs had placed the injector some 3 cm below the substrate, which would interfere with other parts of the chamber, namely the shutter attached to the substrate holding and heating assembly. The injector needed to be within 2.54 cm of the substrate to clear the shutter. This simulation was judged based on the gradient appearance alone, seen in Figure 10.

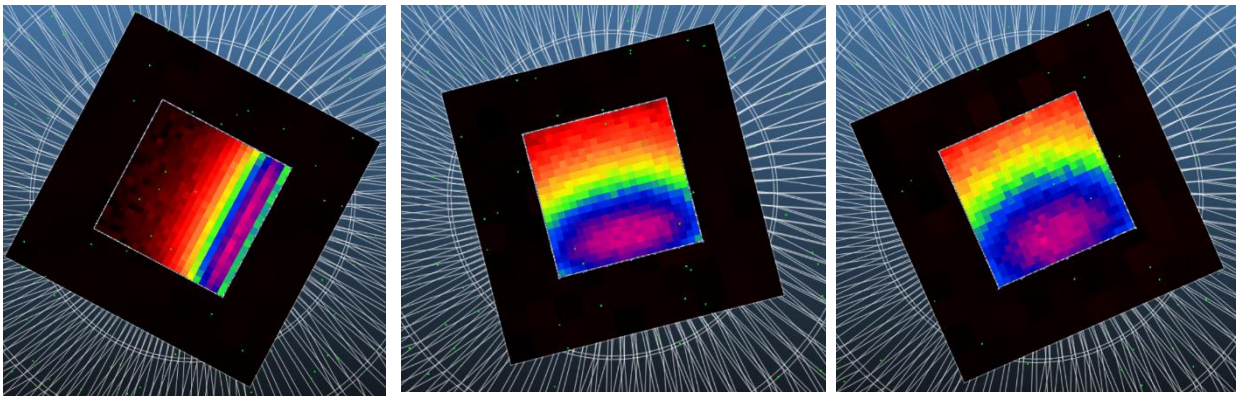

Fig. 10*, substrate pressure gradients for 1 cm, 3 cm, and 4 cm below the substrate*

While there is obvious difference in the severity of the gradient and the overall distribution of the pressure, and thus flux, it was agreed that moving closer to the substrate would not be of any major detriment to the deposition process. This was again in part due to the rotation of the substrate platform.

III.2 Part Design

Usage of alternative sources is well-established in oxide MBE systems, utilizing plasmas, ozone sources, and other oxygen injectors. Alternative (e.g. gaseous) sources of chalcogens like sulfur and selenium are much less established. Thus, oxide systems were used as a starting point for potential designs.

Based on examples from other labs, such as that seen in Figure 12, computational testing was performed for various geometries, settling finally on a linear injector for ease of fabrication.

Early iterations, such as that in Figure 13, featured a line of sources about 3 cm below the

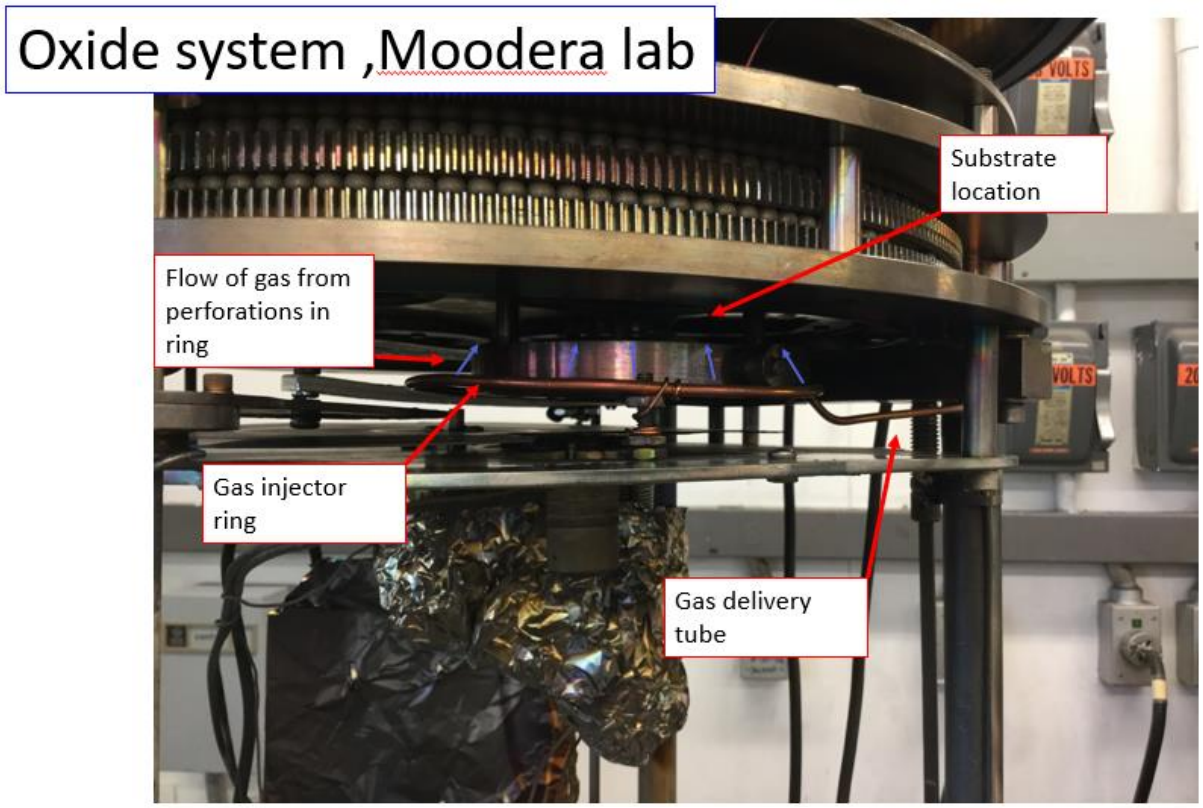

Fig. 12, *Example of ring-based source*

plane of the substrate, directly below the edge of the substrate itself. The line extended the original tubing over a short distance before rising up and back to the level of the sources. The

line then extended forward and ended in a tee with the sources. Various issues arose with this design.

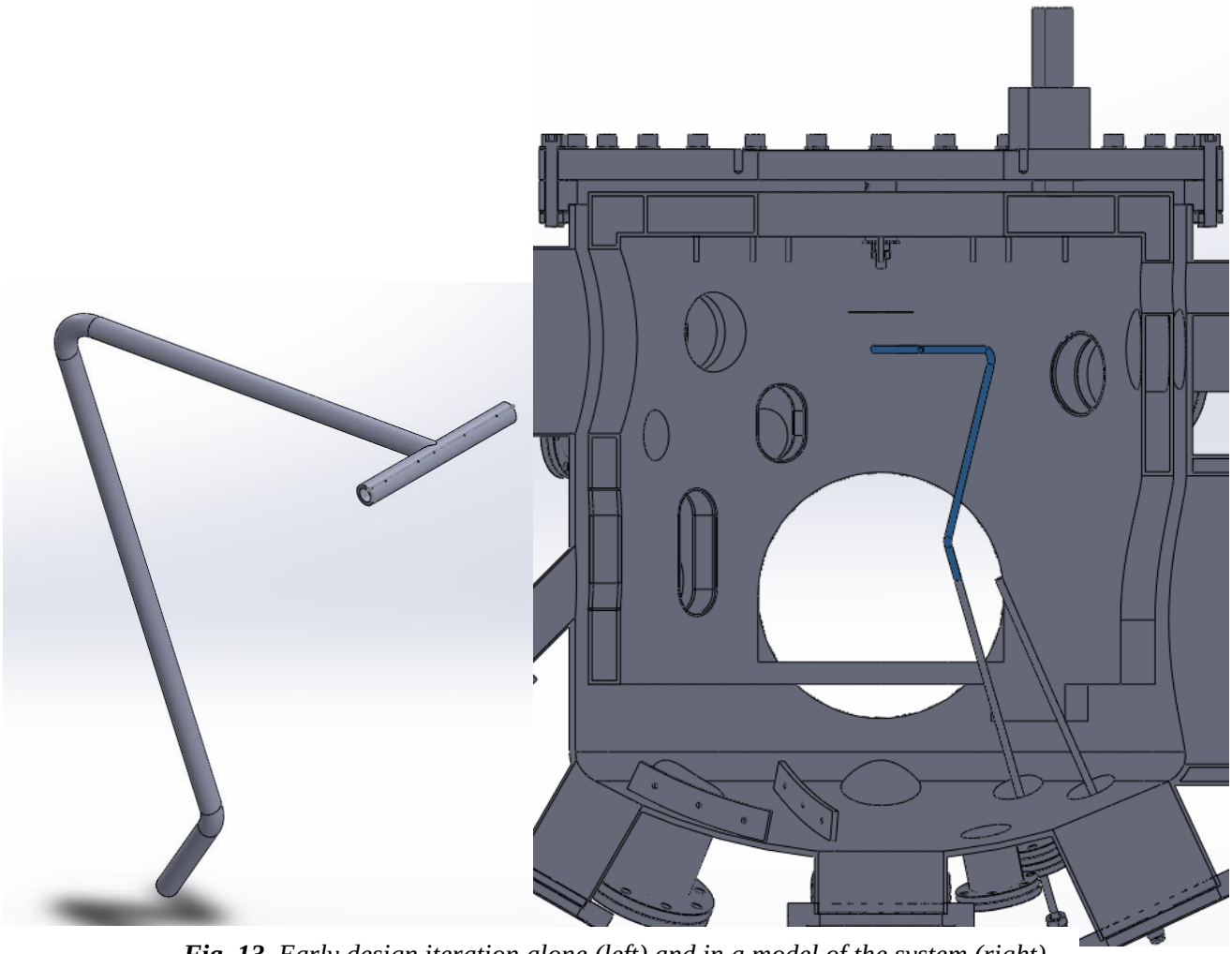

Fig. 13, *Early design iteration alone (left) and in a model of the system (right)*

Unfortunately, the model of the chamber from Mantis, from which I had been basing the path of the tubing, did not include many important elements that actually exist within the chamber, including the diameter of the sample holder and a substrate shutter. I had also failed to consult the port schedule to see if the port directly above the original tubing was used and thus needed to be clear.

Concerns were raised but ultimately dismissed about the injector blocking the upward path from the electron beam evaporator in the lower section of the system. The electron beam

evaporator is installed in the system through the large diameter, horizontal port near the gas sources. The path of the initial designs and all subsequent traveled away from the path of the ebeam and thus posed no issues.

Middle iterations were very conservative about avoiding occupied ports, to the point that they were impractically long, bending to accommodate the straight part of the injector almost as far back as the chamber's cryopanel. It was decided that these types of design (see Figure 14) were overly conservative and that the length could be compressed if it swung back towards the original sources after clearing the support post of the sample shutter.

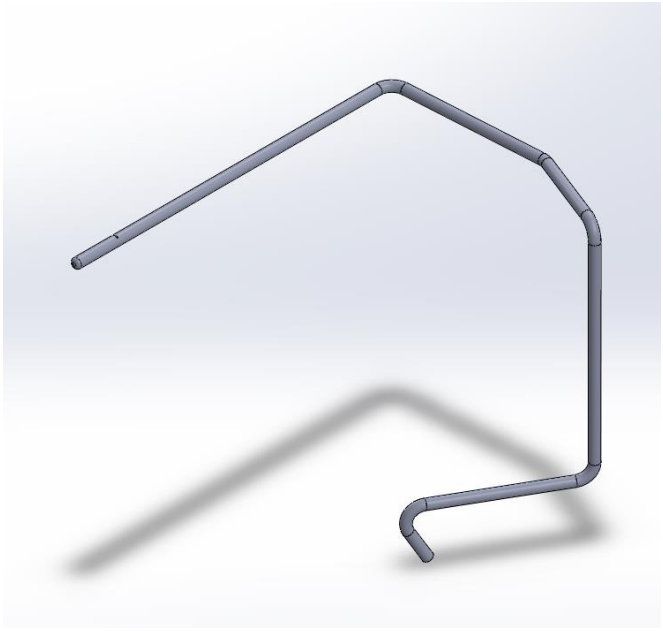

Fig. 14, *Intermediate design iteration*

This resulted in the final designs (Figure 15), which were sent to the central shop for fabrication.

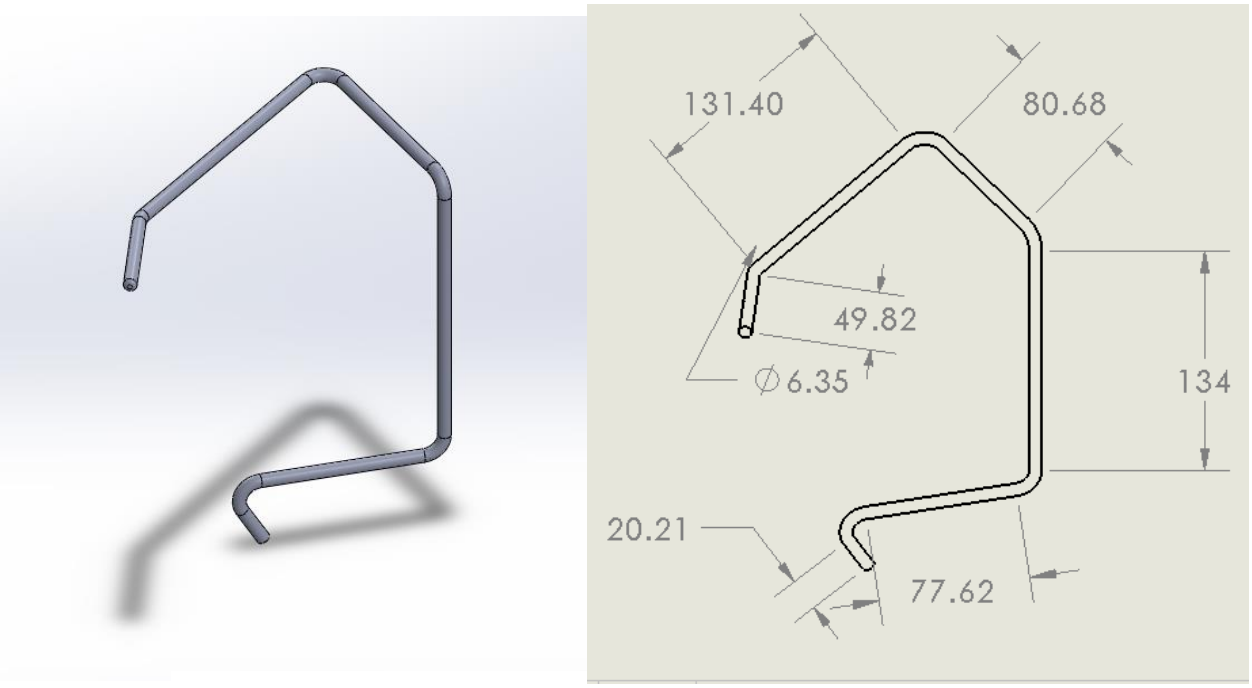

Fig. 15, *One of the final part designs, with dimensions in mm on the right*

III.3 Materials Selection

As described in section II.3, the primary concerns with regards to the composition of the tubing were resistance to corrosion from the gases and resistance to heat up to 1000 C. Secondary concerns were weldability, due to the potential for two different materials being used and also to allow for a cap to be made at the end of the injector.

To this end, the initial ideas, supported by advice from outside sources, were to use some form of Hastelloy for the injector segment and stainless steel for the main length. Repeated discussion with experts from various companies failed to produce particular confidence in the selection of a specific alloy. HR-160 seemed promising, but companies do not make and keep tubing of this material in stock, let alone in the size we needed, ¼". Further, this alloy is hard to work with. Workability and weldability were the reasons why molybdenum was not seriously considered, though that is the material already in use in the existing tubes.

Table 4. *Information informing selection of tubing material*

Material	Ni content	Sulfidation test params	Corrosion rate (mpy)
HR-160[6]	37 balance (wt%)	1100°F, 52.5% H2S atmosphere	14.4
310 SS[7,8]	19-22%	Sulfur vapor, 1060°F for 1295 h	18.9
309 SS[7,9]	12-16%	Sulfur vapor, 1060°F for 1295 h	22.3
Inconel 693[10]	53-68%	No Data	No Data

The nickel content of the alloy is indicated to be a potential source of increased corrosion in H2S and other sulfidating environments.[9] The 309 stainless steel has a lower percentage of nickel than 310 and has a lower corrosion rate, consistent with this information. However, the HR-160 appears to have a larger percentage of nickel than the stainless steels but with a lower

corrosion rate (albeit for different conditions). Additional data in the information sheet for HR-160 shows visually less corrosion than stainless steels in identical conditions[6], so it is likely that something in the processing of the HR-160 is responsible for the improved corrosion resistance, though it is also possible that other composition differences could contribute as well.

Despite the favorable properties of HR-160, it was decided that making the injector out of a different material than the rest of the tubing was inconvenient and likely of more trouble than benefit. Three alloys were then considered: 309 SS, which has preferable resistance to sulfur corrosion; 310 SS, which does well at high temperature but is less resistant to sulfur than 309; and Inconel 693, which was considered a last resort and was difficult to find information on.

309 SS would have been the best choice for the tubing, but contacting companies revealed that it is not a stock item for the relatively small diameter of tubing desired. Fabrication from billet was either too expensive or resulted in too long of a lead time.

Ultimately, 310 SS was selected because the properties were acceptable and the tubing was readily available in ¼" size. While 310 is more corrosion resistant than common varieties of stainless steel, such as 316[7], the most readily available information addresses corrosion from sulfur vapor. The long-term effects of use with hydrogen sulfide gas at elevated temperatures in high vacuum appear to be unknown.

Additionally, the effects of hydrogen selenide gas on 310 SS are virtually absent in the available documentation and literature. That will also be a potential issue in the long-term operation of these modifications.

IV. Conclusion and Future Work

After early experiments using the hydrogen sulfide and hydrogen selenide gas sources in the Jaramillo Group's MBE system failed to generate the desired results, it was suggested that the kinetics of the reactions were inhibiting growth. To improve the rate of reaction, the sources needed to be closer to the substrate to promote collisions.

While a simple linear extension was installed on one of the source lines, a series of computational simulations were done using MolFlow+. These simulations showed that moving the source closer to the substrate would indeed increase the number of collisions, but the allowed linear extensions were insufficient. To get the sources as close as possible, alternate geometries were proposed, and the linear injector was determined to be the best choice.

The linear injector went through an iterative design process, continuously adapting to information not initially considered. The final designs placed the sources within an inch of the substrate, vertically, with one injector on top of the other.

The choice of materials was limited by the available stock of retailers of metal tubing, resulting in a final selection of 310 stainless steel. The long-term impacts of this material selection will need to be monitored, since it may experience corrosion from the hydride gases.

At the time of this writing, the parts had yet to be installed or tested, making those the logical next steps and future work regarding this research.

References

(1) McCray, W. P. MBE Deserves a Place in the History Books. *Nat. Nanotechnol.* **2007**, *2*, 259–261. https://doi.org/10.1038/nnano.2007.121.

(2) Frigeri, P.; Seravalli, L.; Trevisi, G.; Franchi, S. 3.12 - Molecular Beam Epitaxy: An Overview. In *Comprehensive Semiconductor Science and Technology*; Bhattacharya, P., Fornari, R., Kamimura, H., Eds.; Elsevier: Amsterdam, 2011; pp 480–522. https://doi.org/10.1016/B978-0-44-453153-7.00099-7.

(3) Ottesen, V. *English: A Molecular Beam Epitaxy Reaction Chamber Concept Drawing*; 2011.

(4) Molflow documentation | Molflow+ https://molflow.web.cern.ch/content/molflow-documentation-0 (accessed Apr 19, 2019).

(5) Dr. Eberl MBE-Komponenten GmbH. SH200-2S25-S-2108896 Operating Instructions. 2016.

(6) Haynes International. HR-160.

(7) American Iron and Steel Institute. High Temperature Characteristics of Stainless Steel. Nickel Development Institute.

(8) 310 Stainless Steel, 310 SS, UNS S31008, 310 Stainless, Type 310/310S - MEGA MEX http://megamex.com/stainless_310.html (accessed Apr 26, 2019).

(9) North American Stainless. 5.

(10) Super Alloy INCONEL 693 (UNS N06693) https://www.azom.com/article.aspx?ArticleID=9462 (accessed Apr 26, 2019).